LA-UR-97-1036

Title:

Optimization of Densification Modeling Parameters of Beryllium Powder Using a Fuzzy Logic Based Multiobjective Genetic Algorithm

Author(s): Brian J. Reardon

Submitted to:

Optimization Of Densification Modeling Parameters Of Beryllium Powder Using A Fuzzy Logic Based Multiobjective Genetic Algorithm

Brian J. Reardon, Los Alamos National Laboratory, MST-6, Los Alamos, NM 87545

Abstract

A fuzzy logic based multiobjective genetic algorithm (GA) is introduced and the algorithm is used to optimize micromechanical densification modeling parameters for warm isopressed beryllium powder. In addition to optimizing the 19 main parameters of the model with 17 objective functions (experimental data points), the GA provides a quantitative measure of the sensitivity of the model to each parameter, estimates the mean particle size of the powder, and determines the smoothing factors for the transition between stage 1 and stage 2 densification. While the GA does not provide a sensitivity analysis in the strictest sense, and is highly stochastic in nature, this method is reliable and reproducible in optimizing parameters given any size data set and determining the impact on the model of slight variations in each parameter.

1.0 Introduction

1.1 Beryllium Powder Processing

Beryllium and its two most common alloys, beryllium-copper and beryllium-aluminum have a number of interesting properties that make them extremely useful as well as materials of intense study over the past twenty years. These properties include

high elastic modulus, low density, high melting point, high heat capacity, high thermal conductivity, non-magnetic, and superior optical qualities. Consequently, the aerospace industry has found a use for these materials in engines [Marder (1986)], navigational systems [Marder (1984)], and brakes [Paine and Stonehouse (1977)]. The optical field has found a use for beryllium in mirrors [Clement *et al.* (1992)]. Finally, the field of nuclear fusion [Marder *et al.* (1990)] has found numerous uses for these materials. Unfortunately, the cost [$350.00/lb] and potential hazards [Eisenbud (1997); Tinkle (1997)] of beryllium powder has limited its use to situations in which it is absolutely required. Near net or net shape powder processing has shown to be a viable route around these limitations [Marder (1990)]. However, further development is needed to make the technology competitive. Due to the expense and danger involved in this development, computer modeling is a reasonable approach to solving the technological problems at hand.

One common numerical approach to solving these problems lays in the micromechanical modeling method first introduced by Ashby [1972] and further discussed by Artz *et al.* [1983]. This model assumes a random dense packing of monosized spheres that, when subjected to heat and pressure, densify according to the mechanisms of plastic yielding, diffusion, and creep. The utility of such a model is exemplified in the generation of HIP densification maps which show the density achieved by a powder compact under specific conditions along with the corresponding amount of grain growth and the primary densification mechanism involved. Numerous authors are using the micromechanical model as a guide to more efficient HIP

processing of complex shapes [Bingert *et al.*, 1996; Suryanarayanan *et al.*, 1993, 1994].

Unfortunately, there are a number of limitations to the micromechanical modeling procedure. The most obvious is that the quality of the model is limited to the quality of the input data. Another important point is that the quality of the model is not equally influenced by all parameters and it is important to know ahead of time which parameters are most influential as it will be these that are the greatest source of error. Next, the sintering parameters of a powder used in published densification work may be considerably different than those of the powder with which a researcher is working and thus each researcher must be able to optimize the model parameters base on their own densification data. These differences in powders arise from differences in surface chemistries, attrition *vs.* spray forming, size distributions, and morphologies. Finally, the standard micromechanical models assume a random dense packing of monosized spherical particles. However, most particle size distributions are not monosized and attritioned particles are not spherical. Thus, in addition to optimizing the 16 main densification parameters, the ideal particle size used in the model must also be optimized.

There has been a significant amount of work into sensitivity analysis of input parameters for the Ashby model [Suryanarayanan *et al.*, 1993]. Based on the powders studied by these authors, the most influential densification rate model parameters for metals, are the yield stress, power law creep reference stress, the power law creep exponent, and the boundary diffusion coefficient. Most of the other parameters do not significantly influence the densification rate within the temperature and pressure

ranges typically studied. Finally, it should be noted that most tuning of the Ashby HIP parameters is done based on experimental densification data alone and not on grain growth or dominate densification mechanism data, both of which can be obtained from proper microstructural analysis. This is an important point to consider when optimizing parameters since different parameters may fit the densification data equally well but will result in different dominant densification mechanisms and grain growth maps.

An improvement in the micromechanical modeling methods would result in a better understanding of the temperature and pressure schedules needed to achieve full density while at the same time minimizing grain growth. This in turn would save time, materials costs, retooling cost, finishing costs, and environment/worker exposure. This paper presents the results of using a fuzzy logic based multiobjective genetic algorithm to optimize the parameters of beryllium powder[Roberts, 1983].

The fuzzy logic based multiobjective GA methodology was presented elsewhere [Reardon, 1997a, 1997b, 1998]. A brief description follows in the next section.

The micromechanical model being used in this optimization differs from Ashby's HIP 6.1 in a number of ways. The main modification being that in this optimization the micromechanical densification rate equations as well as the grain growth rate equations are solved numerically as a function of time. This results in considerably less accumulation of error than in the numerical solutions as a function of density used by Ashby and Artz in the calculation of densification maps. Since the solving of the equations occurs in two fundamentally different ways between the present study and

Ashby's HIP6.1 (Ashby, 1987), the optimized parameters from this work will not necessarily appear to be most optimal when inserted into HIP 6.1.

In Ashby's micromechanical model, densification is expressed as the instantaneous change in density due to particle yielding, ρ_Y, and the total densification rate, $\dot{\rho}_T$, which is a linear sum of the densification rates due to diffusive mechanisms, $\dot{\rho}_D$, power law creep, $\dot{\rho}_{PLC}$ and Nabarro-Herring creep, $\dot{\rho}_{NH}$. For densities less than ρ_1, which is considered to be an adjustable parameter, the densification equations are:

$$\rho_Y = \left[\frac{P(1-\rho_o)}{1.3\sigma_Y} + \rho_o^3 \right]^{1/3} \qquad \text{Eq. 1.}$$

where P is applied pressure, σ_Y is yield stress, ρ_o is the initial density,

$$\dot{\rho}_D = 32(1-\rho_o)\frac{D_V}{r^2}\tilde{F}_1 + 43\frac{(1-\rho_o)}{(\rho-\rho_o)}\frac{\delta D_B}{r^3}\tilde{F}_1 \qquad \text{Eq. 2.}$$

where r is the particle radius, ρ is the present density, δ is the grain boundary width,

$$\dot{\rho}_{PLC} = 3.1\rho\left[\frac{(1-\rho_o)}{(\rho-\rho_o)}\right]^{1/2} D_C\left[\left[\frac{(1-\rho_o)}{(\rho-\rho_o)}\right]\left[\frac{P-P_o}{3\rho^2\sigma_{REF}}\right]\right]^n \qquad \text{Eq. 3.}$$

where σ_{REF} is the power law creep reference stress, n is the power law creep exponent, P_o is the initial internal pore pressure,

$$\dot{\rho}_{NH} = \frac{14.4}{\rho}\left[\frac{(1-\rho_o)}{(\rho-\rho_o)}\right]^{1/2}\left[\frac{D_V}{G^2} + \frac{\pi\delta D_B}{G^3}\right]\tilde{F}_1 \qquad \text{Eq. 4.}$$

where G is the grain size,

$$\tilde{F}_1 = \frac{(P-P_o)\Omega}{kT} + \frac{3\rho^2(2\rho-\rho_o)\gamma\Omega}{(1-\rho_o)rkT} \qquad \text{Eq. 5.}$$

where k is Boltzman's constant, T is temperature, γ is surface energy, Ω is atomic volume,

$$D_V = D_{OV}\, exp\left(\frac{-Q_V}{RT}\right) \qquad \text{Eq. 6.}$$

where D_{OV} is the volume diffusion pre-exponential factor, Q_V the volume diffusion activation energy, R is the gas constant,

$$\delta D_B = \delta D_{OB}\, exp\left(\frac{-Q_B}{RT}\right) \qquad \text{Eq. 7.}$$

where D_{OB} is the boundary diffusion pre-exponential factor, Q_B the boundary diffusion activation energy,

$$D_C = 10^{-6}\, exp\left(\frac{-Q_C}{RT_M}\left(\frac{T_M}{T} - 2\right)\right) \qquad \text{Eq. 8.}$$

where T_M is the melting temperature, Q_C the power law creep activation energy.

For densities greater than ρ_2 which is also considered to be an adjustable parameter the densification rate equations are:

$$\rho_Y = 1 - exp\left[\frac{3P}{2\sigma_Y}\right] \qquad \text{Eq. 9.}$$

$$\dot{\rho}_D = 3\left[\frac{1-\rho}{6\rho}\right]^{1/3}\frac{D_V}{r^2}\tilde{F}_2 + 4\frac{\delta D_B}{r^3}\tilde{F}_2 \qquad \text{Eq. 10.}$$

$$\dot{\rho}_{PLC} = 1.5\rho(1-\rho)D_C\left[\frac{1.5(P - P_1)}{n\sigma_{REF}\left(1-(1-\rho)^{1/n}\right)}\right]^n \qquad \text{Eq. 11.}$$

$$\dot{\rho}_{NH} = 32(1-\rho)\left[\frac{D_V}{G^2} + \frac{\pi\delta D_B}{G^3}\right]\tilde{F}_2 \qquad \text{Eq. 12.}$$

$$\tilde{F}_2 = \frac{(P - P_1)\Omega}{kT} + \frac{2\gamma\Omega}{rkT}\left[\frac{6\rho}{1-\rho}\right]^{1/3} \qquad \text{Eq. 13.}$$

$$P_1 = \left[\frac{1-\rho_c}{1-\rho}\right]\frac{\rho}{\rho_c}P_o \qquad \text{Eq. 14.}$$

where ρ_c is the critical density at which pores become closed.

For densities falling between ρ_1 and ρ_2 the above equations (2-4 and 10-12) are scaled accordingly and summed to give the total densification rate.

1.2 Nonlinear curve fitting

Generally speaking, one can formulate any optimization problem into a single standard of measurement - a cost function or a fitness function - that determines the performance of a decision and then recursively improves the performance by selecting from the most feasible of alternatives. A typical scenario in nonlinear parameter optimization would involve minimizing the least squares difference between all the data points of a calculated and experimental densification curve (density *vs*. temperature or density *vs*. pressure). In other words, to minimize the quantity:

$$\Phi = \left|\frac{1}{N}\sum_{i=1}^{N}\left(\rho_{Ei} - \rho_{Ci}\right)^2\right|, \qquad \text{Eq. 15.}$$

where N is the number of data points, ρ_{Ei} is an experimental data point, and ρ_{Ci} the calculated densification point. Traditional deterministic optimization techniques require the use of gradient or higher order statistical analysis of Φ:

$$\frac{\partial \Phi}{\partial a} = \frac{2}{N}\sum_{i=1}^{N}\left(\rho_{Ei} - \rho_{Ci}\right)\frac{\partial \rho_{Ci}}{\partial a} = 0 \qquad \text{Eq. 16.}$$

for each variable, *a*, being optimized.

Such an approach can only handle the optimization of one densification curve at a time and typically does not properly account for the uncertainty that is inevitably present in the experimental data. To complicate matters, complete densification curves are not always readily available. Instead, individual density points at various temperatures and pressures are usually the most common form of densification data.

The fuzzy logic based multiobjective GA, as described in previous papers [Reardon], is ideally suited to overcoming these deficiencies. First, the GA treats each individual data point as a separate objective to which the model parameters must be optimized and thus there is no need for smooth experimental densification curves. Second, there is no limit to the number of objectives or parameters that can be operated on at one time. Third, the use of fuzzy rule sets to determine the most optimal of parameters allows for one to incorporate experimental error.

1.3 The Genetic Algorithm

Darwinian evolution is an intrinsically robust search and optimization procedure. Evolved biota have optimized solutions to complex problems at every level of organization, from the cell up to the population. The problems that biota have solved and continue to improve upon, are typified by chaos, chance, temporality, nonlinearity, and multidimensionality. Such problems have proven to be intractable to

deterministic optimization techniques, especially in situations where heuristic solutions are not available.

A GA falls into the much broader category of evolutionary algorithms. These algorithms attempt to simulate the processes of evolved biota in optimization. The essence of such a simulation lies in the expression of a solution to a problem not as a single value but as a string of fundamental building blocks (genes) that can be manipulated in much the same way as an extant species will manipulate its gene pool through selection and mating to produce more optimal offspring for the current environment. For example, consider x_1, which is a member of a population of feasible solutions to a problem but not necessarily the optimal solution. The real value of x_1 is expressed as a string of binary digits, *e.g.*: 101101110, that is L digits long. This binary string is mapped to a real value of x_1 such that the string 11111111 corresponds to x_{max} and 00000000 corresponds to x_{min}. x_{max} and x_{min} define the upper and lower bounds respectively of the range of x that is being searched. The real value of x_1 is commonly referred to as a phenotype. If a function requires the optimization of more than one variable, $f(x,y)$, then the total string for a specific member is formed by placing the binary digits defining x and y back to back in one string. For example if x_1=001100 and y_1 = 110001 then the string for member #1 would be: 001100110001.

Manipulation of these strings occurs in much the same way as extant species manipulate chromosomes. First, competition among members of the population determines who is most fit or optimal. Second, the most optimal members are allowed to reproduce. Reproduction involves slicing the chromosomes of two members of the populations and then exchanging the segments:

$$\begin{array}{l} X_1 : 10100011 \\ X_2 : \underline{11110111} \end{array} \rightarrow \begin{array}{l} \tilde{x}_1 : 1010\underline{0111} \\ \tilde{x}_2 : \underline{1111}0011 \end{array}$$

$\tilde{x}_1$ and $\tilde{x}_2$ are the resulting progeny and will be placed in the next generation. The actual crossover site is selected randomly with some probability, p_c. Third, mutation occurs, which in a positively entropic system ensures genetic diversity in the subsequent generation. Mutation involves flipping the value of a randomly selected bit with some probability, p_m. The new population that evolves from the selection, crossover, and mutation operators is defined as a generation. This cycle is repeated for a number of generations as specified by the user.

Multiobjective optimization using fuzzy logic can be summarized in two steps. First, a single fitness value that incorporates the values of all the objectives is calculated using fuzzy rule sets. Second, two randomly selected members are compared to a comparison set. If one member has a fuzzy fitness value that dominates the set and the other does not then the dominating member is selected. Otherwise, continuously updated phenotypic niching is incorporated.

The key to the fuzzy logic approach lays in the definition of the fitness function and its corresponding fuzzy rules:

$$F = \frac{1}{N}\sum_{i=1}^{N} f'\left(f_i\right) \qquad \text{Eq. 17.}$$

which is essentially an average over the N objectives in question. *f'* is a fuzzy logic rule set that scales the objective, f_i, according to how far away it is from the experimentally optimal solution. A typical fuzzy set would have the form:

$$\text{if } f_i \le (O_i - E_i) \rightarrow f'(f_i) = \left(\frac{S_{\min}}{f_{i\min} - (O_i - E_i)} \right) \left(f_i - (O_i - E_i) \right) \qquad \text{Eq. 18a.}$$

$$\text{if } (O_i - E_i) \le f_i \le (O_i + E_i) \rightarrow f'(f_i) = 0 \qquad \text{Eq. 18b.}$$

$$\text{if } f_i \ge (O_i + E_i) \rightarrow f'(f_i) = \left(\frac{-S_{\max}}{(O_i + E_i) - f_{i\max}} \right) \left(f_i - (O_i + E_i) \right) \qquad \text{Eq. 18c.}$$

where O_i is the ith experimental value that the ith function, f_i, is being optimized towards, E_i is the error or accepted uncertainty in O_i, $S_{min(max)}$ is a scaling parameter for values below (above) the accepted value, $f_{imin(imax)}$ is the smallest (largest) value of all the *i*th objectives in the population.

1.4 Defining the upper and lower bounds of the search space

The efficiency of all optimization techniques is greatly enhanced when reasonable limits are placed on the search space. The fuzzy logic based GA is no exception and to that end, the Ashby's HIP Users Manual [Ashby, 1990b] and references therein provides limits for all of the parameters to be optimized.

1.5 Densification curve sensitivity to parameter values

The stochastic nature and large population size of a fuzzy logic based multiobjective GA provides a distribution of feasible answers to a problem. Thus, parameters that are not very important (*i.e.*: do not have a significant impact on the objective values will have a broad, almost random, distribution and parameters that do significantly impact the objective values will have a narrow distribution.

Thus, the final optimized population provided by a GA provides insight to the sensitivity of the parameters on the models. Formal sensitivity analysis has been conducted previously [Suryanarayanan *et al.*, 1993, 1994]. This work reveals that in many metals, such as that of copper powder, the yield stress and the parameters of the power law creep mechanism are the most influential factors in the densification model. Thus, if the fuzzy logic based GA operates as expected, the optimized population will show these parameters to have a narrow distribution and the other parameters to have a much broader or random distribution.

2.0 Procedure

The first step in fuzzy logic based GA optimization, is to determine the parameter range to be searched. Table I lists the range for each parameter. In addition to the densification mechanism parameters themselves, the fuzzy logic GA will also be optimizing the particle size and the smoothing parameters that control the transition between stage 1 and stage 2 densification.

The smoothing function operates in the following way: If the current density, ρ, is greater than or equal to the stage 2 cut off density, ρ_2, then the stage 2 densification rate equations are calculated and multiplied by a weighting factor (s1) that is determined by: $s1 = (\rho - \rho_2)/ (1. - \rho_2)$.

Likewise, if the current density is less than or equal to the stage 1 cut off density, ρ_1, then the stage 1 densification rate equations are calculated and multiplied by a weighting factor that is determined by: $s1 = 1 + ((\rho_o - \rho)/ (\rho_1 - \rho_o))$, where ρ_o is the initial density of the powder. All of the weighted densification rates are then added to give a total densification rate.

The second step is defining the objectives to be optimized. In this work, the goal is to minimize the difference between the calculated densification values and the densification data points of each of the several experimental studies available within a specified experimental error. The actual experimental error was not available in any of the original work and thus it had to be approximated. Table II lists the objective conditions of the data set along with experimental error estimated by the present author. Note that the GA will only calculate the densification data for these points and not the entire densification map. Also, the exact heating and pressure schedules were not available in Roberts' report. Thus, it was assumed that the temperature and pressure were ramped over 500s to the temperatures and pressures reported by Roberts and then held for 1 hour.

The third step is to define parameters of the GA itself. Table III lists the parameters of the GA used in this optimization.

3.0 Results and Discussion

The stochastic nature of a GA optimization requires multiple runs to ensure reproducibility. Thus, for this work, the GA was run four times and each time similar results were obtained. Figures 1a and 1b show the fitness averaged over the entire population and the associated standard deviation for two objective functions from the data set of Roberts. All of the objective functions behaved in a similar fashion in that their absolute values were minimized and the standard deviation decreased with generation number indicating convergence. As indicated in Figures 1a and 1b some of the objectives were minimized to zero whereas others were minimized to a value other than zero. Furthermore, as indicated by the standard deviation in Figure 1b, there were members of the population that solved the objective well in early generations but the GA eventually evolved towards solutions that were less optimal . The reason for this lays in the fact that all of the objectives were being optimized simultaneously. Thus, while a member in an early generation of Figure 1b may have been optimal in solving one particular objective, it was not optimal in solving all of the objectives in question. The mandate of the fuzzy logic based multiobjective GA is to find the best of all possible tradeoffs between all the objectives in question and thus, for the objective in Figure 1b, a slightly less than optimal solution satisfies that mandate. The final convergence of the population towards an objective value that was clearly not as optimal in Figure 1b as in other objectives results from one of two conditions. First, the model may be lacking in its ability to properly simulate the densification mechanisms of this powder at this density, time, pressure and

temperature. Second, the experimental error, which was not reported by Roberts, may be large enough to encompass the calcualted value within one standard deviation.

The model parameters being optimized behave in a similar manner from run to run. Figures 2a and 2b show the evolution of two of the 19 parameters (16 model parameters, the particle size, and 2 cutoff densities) while optimizing with Robert's data set. As is typical of metal powders, the yield stress and power law creep mechanisms seem to be the most sensitive parameters and thus tend to converge most quickly. Other parameters, such as the surface energy, however, do not converge quickly because they do not have a significant impact on the model.

Once the optimization is complete, a member of the population can be selected based on its ability to minimize the objective functions to be used in the micromechanical model for the calculation of densification maps. A mulitobjective optimization technique such as this finds a distribution of feasible solutions to a problem. Thus, with the exception of an occasional member who is clearly not optimal due to a random mutation, all of the remaining members are optimal. In other words, though the members may have different parameter values, they all solve the problem as defined and thus no one member can be considered better fit than any of the others. This fact is shown in Table IV where the average parameter values, standard deviations, and sensitivities are listed. The sensitivity parameter is determined by normalizing the parameter search space range with the standard deviation. The rather large standard deviations and low sensitivity of some of the parameters indicate that there exists a broad distribution of acceptable solutions to the problem at hand.

A cautionary note is in order here. The GA used only the densification data available to optimize the parameters. Thus, while the parameters of interest fit the data present, the rest of the densification and grain growth maps may differ substantially depending on the member of the population that is selected. The diversity of optimized parameter values are shown in Table V. Table V shows five members of the optimized population that all solve the objectives equally well but have different parameter values.

Figure 3 shows the relative density *vs.* sintering time for the 5 samples listed in Table V. This calculation involved a ramping of the temperature and pressure from 0.1MPa and 293K at t=0 to 15.168MPa and 973K within 500s. The temperature and pressure were then held constant for an additional 3600s and then ramped down to ambient conditions in 500s. Even though each member had different parameter values they produced close to the same final density. Note that the majority of densification occured in the first 500s of the ramp up phase of the schedule. Since no details of Roberts' original schedule are available (only his hold times), it is possible that different parameter values could have been obtained if a different ramping schedule was used. This ambiguity would then indicate that experimental densification data would be better used if detailed heating and cooling schedules were provided along with the hold times and experimental error.

The physical values of the parameters listed in Table V and the sensitivity parameters of Table IV merit some discussion. According to Table V, the most influential parameters are the yield stress and the temperature dependence of the yield. According to the optimization, the average optimal yield stress is 970MPa with a

temperature dependence of 2.3. However, other sources (Ablen and Mataya, 1993; Ablen and Osborn, 1994) have reported values of 600MPa with a temperature dependence of 1.16. Likewise the activation energies for diffusion found in this optimization are slightly higher than those previously reported. These observations are consistent with the fact that the powder under study by Roberts was attrition milled. Attrition milled powder is extremely work hardened which would result in a high yield stress and a high temperature dependence of the yield due to an enhanced proclivity towards recrystallization and dislocation movement upon heating. Likewise, attrition milled powder is notorious for its high BeO content on the particle surfaces. The refractory nature of BeO hinders the diffusion of beryllium and thus increases the effective activation energy of diffusion of the powder. The effects of BeO on the parameters of the micromechanical modeling of beryllium was previously addressed (Stoev *et al.*, 1995). In Stoev's work, effective diffusion coefficients were developed to account for the hindering effect of BeO on beryllium diffusion. The net result, as implied in the present work, was to decrease the value of diffusion coefficients or increase the activation energy barrier. Thus, without explicitly stating in mathematical terms the effects of a BeO layer on the particles, the GA was able to adjust the available parameters accordingly to create effective activation energies for diffusion through an oxide layer.

4.0 Conclusions

A fuzzy logic based multiobjective genetic algorithm, as presented in earlier papers, was used to optimize the micromechanical model parameters of beryllium

powder based on the densification data of Roberts. This procedure determined the optimal values of the 19 main parameters as well as the relative impact each parameter has on the final densification model. In addition to showing that the fuzzy logic GA is capable of finding multiple solutions to a multi-objective (17), multi-variable (19) problem, this work has also shown the importance of having a large objective data set on hand along with a realistic assessment of experimental error and process schedules.

5.0 Acknowledgments

Funded by the U.S. Department of Energy and Los Alamos National Laboratory which is operated by the University of California under contract number W-7405-ENG-36.

6.0 References

Abeln, S. P., Mataya, M. C., JOWAG 22B, Beryllium Science & Technology Exchange, Rocky Flats Plant, May 1993.

Abeln, S. P., Osborn, D. W., 'Evaluation of Computer Models for Consolidation of Beryllium Powder,' Internal DOE Report, 1994.

Ashby, M. F., 'A First Report On Deformation - Mechanism Maps,' Acta Metallurgica, 20, 1, 887, 1972.

Ashby, M. F., 'Hip - Maps Software And Operating Manual,' Cambridge University Engineering Department, Cambridge, Uk, 1987.

Ashby, M. F., 'Hip 6.0 Background Reading And Operator Manual,' Engineering Department, Cambridge, U. K., 1990

Arzt, E., Ashby, M. F., Easterling, K. E., 'Practical Applications Of Hot-Isostatic Pressing Diagrams : 4 Case Studies,' Metallurgical Transactions A-Physical Metallurgy And Materials Science, 14a, 2, 211-221, 1983.

Bingert, S. R., Vargas, V. D., Sheinberg, H., 'Tantalum Powder Consolidation, Modeling And Properties,' Tantalum, Ed. E. Chen, A. Crowsen, The Minerals, Metals and Materials Society, p. 95, 1996.

Clement, T. P., Parsonage, T. B., Kuxhaus, M. B., 'Near-net-shape Processing Cuts Costs Of Beryllium Optics,' Advanced Materials & Processes, 3, 37, 1992.

Eisenbud M., Kotin P., Miller F., Rogers A., Trichopoulos D., Deubner D. C., Powers M., Emly M., Hanes H., Stonehouse J., Wilson P., 'Is Beryllium Carcinogenic In Humans,' Journal Of Occupational And Environmental Medicine, 39, 3, 205-208, 1997.

Marder, J. M., 'Beryllium in Stress - Critical Environments,' J. Materials For Energy Systems, 8, 1, 17, 1986.

Marder, J. M., 'Beryllium - Technology and Applications,' Journal of Metals, p. 45, June 1984.

Marder, J. M., Kuxhaus, M. B., Stonehouse, A. J., 'Near Net Shape Beryllium Products,' The International Journal of Powder Metallurgy, 26, 2, 139, 1990.

Paine, R. M., Stonehouse, A. J., 'A Corrosion Protection System For Beryllium In Aircraft Brake Applications,' Materials Performance, 27, August 1977.

Reardon, B. J., ‘Fuzzy Logic Vs. Niched Pareto Multiobjective Genetic Algorithm Optimization: Part I: Schaffer’s F2 Problem,’ LA-UR-97-3675, Los Alamos National Laboratory, Los Alamos, N M, 1997a.

Reardon, B. J., ‘Fuzzy Logic Vs. Niched Pareto Multiobjective Genetic Algorithm Optimization: Part I I: A Simplified Born Mayer Problem,’ LA-UR-97-3676, Los Alamos National Laboratory, Los Alamos, N M, 1997b.

Reardon, B. J., ‘Optimization Of Micromechanical Densification Parameters For Copper Powder Using A Fuzzy Logic Based Multiobjective Genetic Algorithm,’ LA-UR-97-0419, Los Alamos National Laboratory, 1998.

Roberts, D., ‘The Warm Isopressing of Beryllium Powder, in ‘Beryllium Science (U),’ JOWOG 22 / AVIS 522, Ed. J. E. Hanafee, UCRL-89338, Vol. 2, p. 176, 1983.

Stoev, P. I., Parirov, I. I., Tikhinskii, G. F., Vasil’ev, A. A., ‘Hot-Isostatic-Pressing Diagrams for Fine-Particle Beryllium Powders,’ Inorganic Materials, 31, 7, 839-844, 1995.

Suryanarayanan, R, Sastry, S. M. L., Jerina, K. L., ‘Consolidation Of Molybdenum Disilicide Based Materials By Hot Isostatic Pressing (HIP) : Comparison With Models,’ Acta Metallurgica Et Materialia, 42, 11, 3741-3750, 1994.

Suryanarayanan, R., Sastry, S. M. L., Jerina, K. L., ‘On The Values Of Material Property Data Used In Hot Isostatic Pressing Models,’ Scripta Metallurgica Et Materialia, 28, 7, 797-802, 1993.

Tinkle S. S., Kittle L. A., Schumacher B.A., Newman L. S., ‘Beryllium Induces Il-2 And Ifn-Gamma In Berylliosis,’ Journal Of Immunology, 158, 1, 518-526, 1997.

7.0 Tables

Table I. Search range for each parameter in the micromechanical model being optimized by the Fuzzy Logic based GA. (PLC: Power Law Creep)

Parameter	Units	Lower Bound	Upper Bound
surface energy	J/m^2	1.5000	2.5000
yield stress	MPa	10.000	1500.0
Temperature Dependence of Yield		0.10000	2.7000
PLC Exponent		5.0000	12.000
PLC Reference Stress	MPa	1900.0	2600.0
PLC Activation Energy	kJ/mol	900.00	1300.0
Low T. to High T. Creep Transition	K	500.00	800.00
C for Low T. Creep		0.50000	0.71000
Pre-exponent for Volume Diffusion	m^2/s	1.0000e-05	3.0000e-05
Activation Energy for Volume Diffusion	kJ/mol	110.00	400.00
Pre-exponent for Boundary Diffusion	m^2/s	3.0000e-15	5.0000e-15
Activation Energy for Boundary Diffusion	kJ/mol	75.000	125.00
Pre-exponent for Surface Diffusion	m^2/s	1.1000e-12	2.0000e-10
Activation Energy for Surface Diffusion	kJ/mol	110.00	250.00
Pre-exponent for Boundary Mobility	m^2/s	1.0000e-15	3.0000e-15
Activation Energy for Boundary Mobility	kJ/mol	100.00	200.00
Particle size Radius	m	2.0000e-05	3.5000e-05
Stage 2 cut off relative density		0.70000	0.99000
Stage 1 cut off relative density		0.70000	0.99000

Table II. The experimental values of warm isopressed Beryllium powder consolidation from Roberts used in the optimization. The optimization assumes a 500s ramp up from 293K and 0.1 MPa, a 3600s hold, and a 500s ramp down to ambient temperature and pressure.

Time (s)	Temperature (K)	Pressure (MPa)	Relative Density	Est. Error
3600.0	873	0.1	0.78	0.005
3600.0	873	55.158	0.81	0.005
3600.0	873	82.737	0.91	0.005
3600.0	923	0.1	0.78	0.005
3600.0	923	15.168	0.80	0.005
3600.0	923	38.611	0.84	0.005
3600.0	948	0.1	0.78	0.005
3600.0	948	31.026	0.80	0.005
3600.0	948	42.058	0.92	0.005
3600.0	948	48.267	0.95	0.005
3600.0	973	0.1	0.78	0.005
3600.0	973	6.895	0.80	0.005
3600.0	973	14.479	0.83	0.005
3600.0	973	15.168	0.84	0.005
3600.0	973	27.579	0.90	0.005
3600.0	973	38.611	0.91	0.005
3600.0	973	55.158	0.97	0.005

Table III. The GA parameters used in the optimization.

Binary string length for each variable	14
Number of generations per optimization	100
Population size	300
Mutation Probability	0.1%
Crossover Probability	90%
Comparison set Size	1

Table IV. The average parameter value and associated standard deviations after 25 generations along with the resulting degree of sensitivity the objective has to each parameter..

Parameter	$\bar{x}$	σ_x	$\frac{(x_{max} - x_{min})}{\sigma_x}$
surface energy	2.0050	0.19990	5.0025
yield stress	968.50	44.500	33.483
T. Dep. of Yield	2.3360	0.13770	18.882
PLC Exponent	8.8440	1.0490	6.6730
PLC Ref. Stress	2208.0	222.40	3.1475
PLC Act. Engy	1149.0	108.70	3.6799
Low T. - High T.	714.60	41.300	7.2639
C for Low T. Creep	0.59280	0.047640	4.4081
Pre-exp. V. Diff.	2.1240e-05	6.0090e-06	3.3283
Act. Engy V. Diff.	292.30	66.290	4.3747
Pre-exp. B. Diff.	3.8390e-15	6.3020e-16	3.1736
Act. Engy B. Diff.	108.80	15.730	3.1786
Pre-exp. S. Diff.	8.3180e-11	6.4710e-11	3.0737
Act. Engy S. Diff.	180.70	39.320	3.5605
Pre-exp. B. Mob.	1.9740e-15	6.5530e-16	3.0520
Act. Engy B. Mob.	135.50	37.470	2.6688
Particle radius	2.7310e-05	4.5000e-06	3.3333
stage 2 cutoff den.	0.84310	0.080430	3.6056
stage 1 cutoff den.	0.93690	0.054710	5.3007

Table V. Five example member's parameter values and the associated objective values produced after the 25th generation of the optimization.

	Sample 1	Sample 2	Sample 3	Sample 4	Sample 5
surface energy	1.9480	2.3380	1.8210	2.0260	2.3210
yield stress	971.90	972.20	953.70	972.20	972.20
T. Dep. of Yield	2.3470	2.3470	2.3470	2.3470	2.3470
PLC Exponent	8.4620	10.350	8.5590	8.6810	8.2130
PLC Ref. Stress	2023.0	2014.0	2001.0	2074.0	2247.0
PLC Act, Engy	976.40	1089.0	1264.0	1026.0	972.90
Low T. - High T.	682.70	762.00	799.50	676.60	700.80
C for Low T. Creep	0.57560	0.65860	0.63180	0.57560	0.59190
Pre-exp. V. Diff.	1.4990e-05	1.4990e-05	1.4990e-05	1.7270e-05	2.2470e-05
Act. Engy V. Diff.	283.40	252.30	252.30	336.90	352.90
Pre-exp. B. Diff.	3.0110e-15	4.3120e-15	4.3120e-15	3.8150e-15	3.4260e-15
Act. Engy B. Diff.	124.60	124.20	124.20	110.90	119.80
Pre-exp. S. Diff.	9.7700e-12	2.5180e-11	2.5180e-11	1.2560e-10	1.6350e-11
Act. Engy S. Diff.	177.20	152.10	145.60	244.80	214.90
Pre-exp. B. Mob.	2.2240e-15	1.0770e-15	2.7970e-15	2.5690e-15	2.1620e-15
Act. Engy B. Mob.	148.00	102.30	109.40	148.00	132.30
Particle radius	2.3290e-05	3.1780e-05	2.7700e-05	2.2320e-05	3.3040e-05
stage 2 cutoff den.	0.84980	0.87830	0.82500	0.74400	0.90170
stage 1 cutoff den.	0.91530	0.96570	0.95530	0.95390	0.98630
Objective 1	7.486e-05	7.486e-05	7.629e-05	2.106e-04	7.480e-05
Objective 2	8.383e-03	8.387e-03	9.927e-03	8.387e-03	8.370e-03
Objective 3	-7.498e-02	-7.497e-02	-7.309e-02	-7.497e-02	-7.499e-02
Objective 4	1.826e-04	1.828e-04	2.346e-04	3.982e-04	1.826e-04
Objective 5	6.513e-03	6.534e-03	1.005e-02	6.534e-03	6.503e-03
Objective 6	1.778e-03	1.823e-03	7.247e-03	1.823e-03	1.759e-03
Objective 7	4.767e-04	4.765e-04	4.858e-04	6.490e-04	4.765e-04
Objective 8	9.039e-02	9.060e-02	9.236e-02	9.060e-02	9.036e-02
Objective 9	3.734e-03	4.138e-03	6.711e-03	4.138e-03	3.683e-03
Objective 10	-9.616e-03	-9.278e-03	-7.124e-03	-9.278e-03	-9.658e-03
Objective 11	4.767e-04	4.765e-04	6.663e-04	6.949e-04	4.765e-04
Objective 12	1.118e-02	1.117e-02	1.560e-02	1.117e-02	1.117e-02
Objective 13	1.084e-02	1.082e-02	1.701e-02	1.082e-02	1.082e-02
Objective 14	3.292e-03	3.272e-03	9.578e-03	3.272e-03	3.272e-03
Objective 15	-1.820e-02	-1.823e-02	-1.023e-02	-1.823e-02	-1.823e-02
Objective 16	2.455e-03	2.403e-03	1.071e-02	2.403e-03	2.403e-03
Objective 17	-1.456e-02	-1.460e-02	-9.356e-03	-1.460e-02	-1.460e-02

8.0 Figures

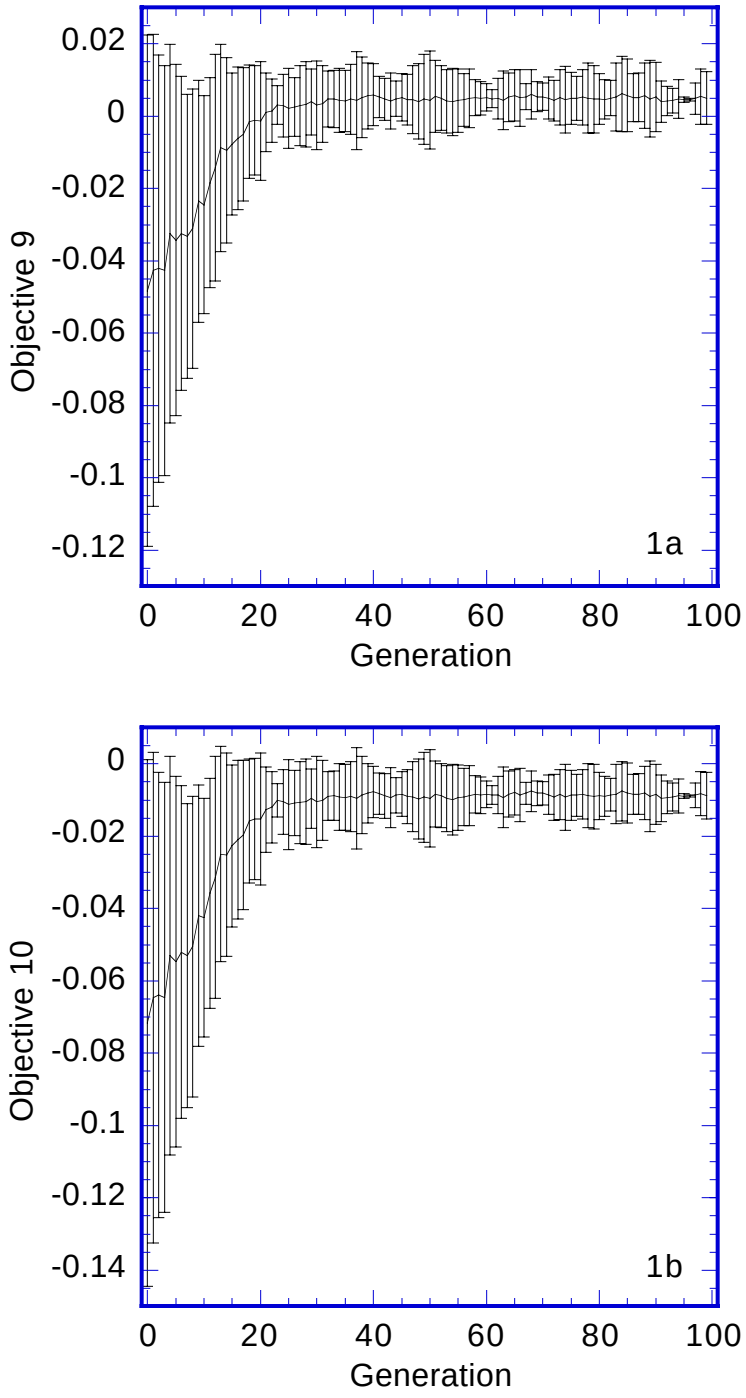

Figures 1a-b. The fitness averaged over the entire population and the associated standard deviation for two of the sixteen objective functions.

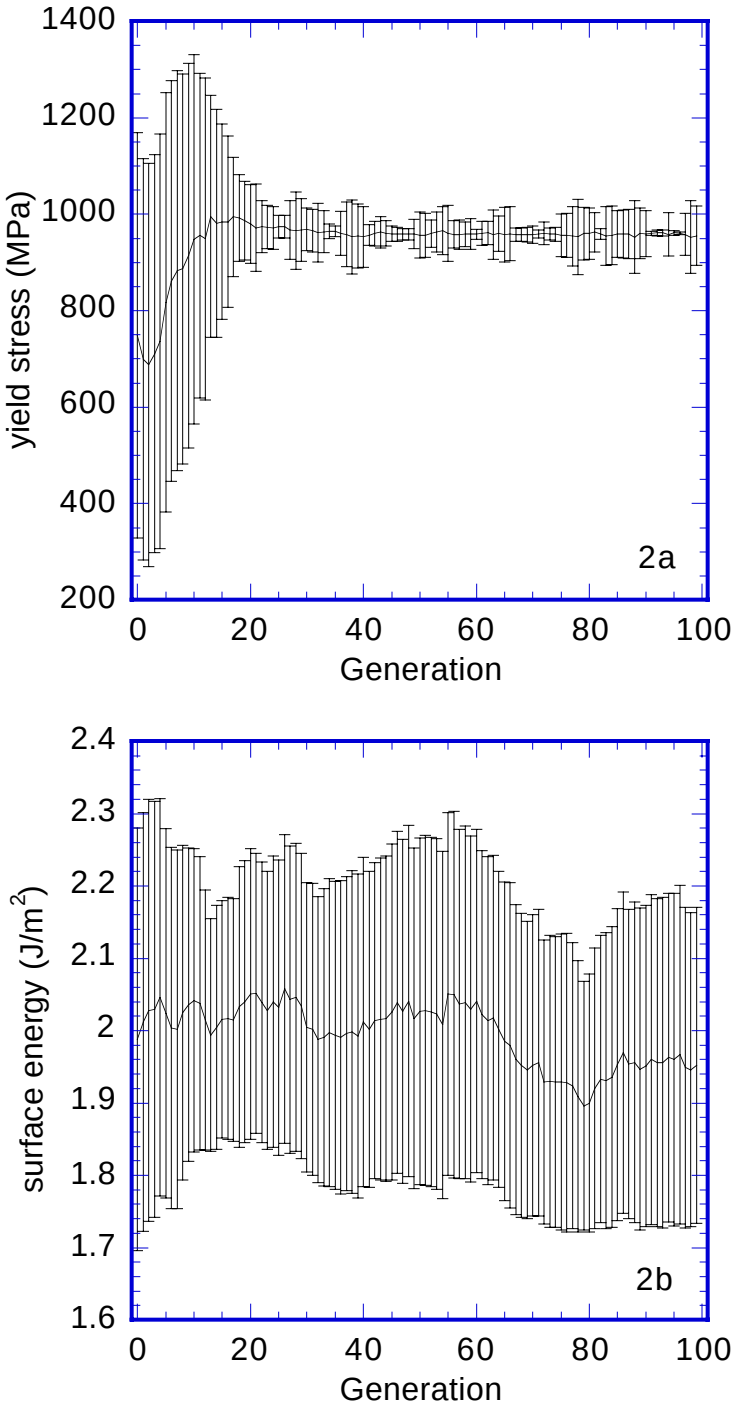

Figure 2a-b. The evolution of the yield stress and the surface energy averaged over the entire population with the associated standard deviations. The yield stress converges indicating that it is an important parameter whereas the surface energy does not, indicating that it is not as significant.

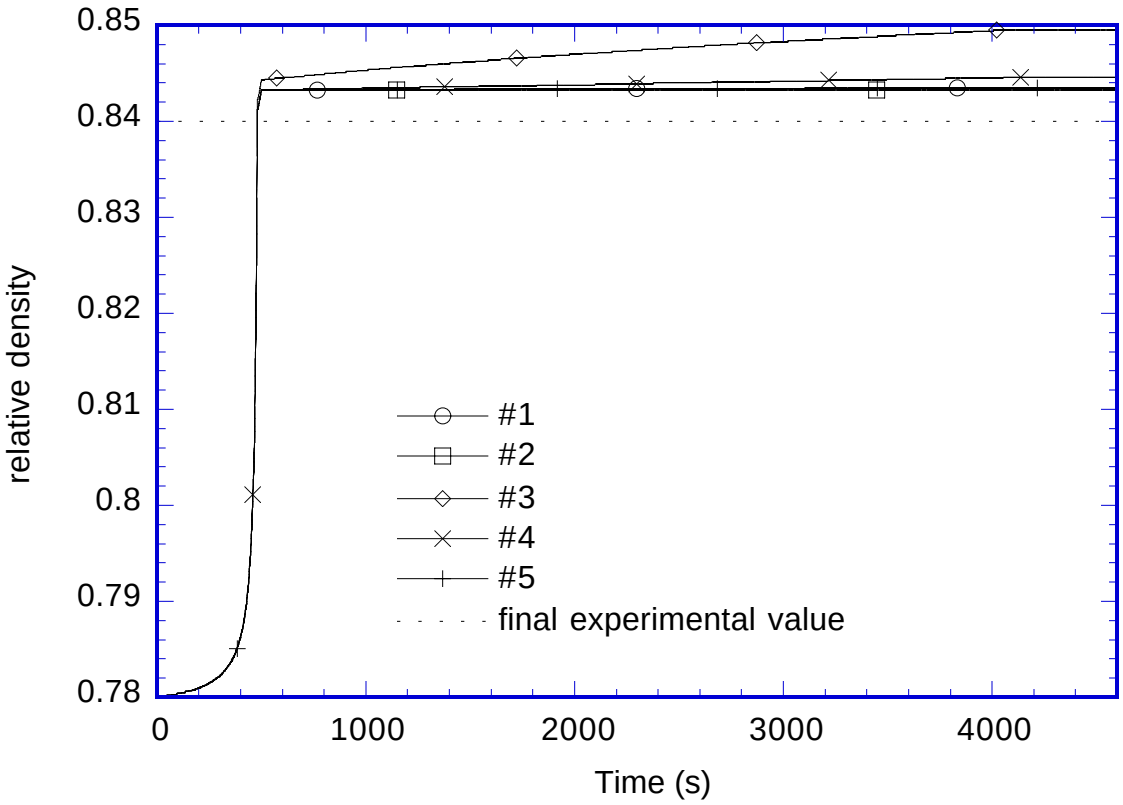

Figure 3. The Relative density v. sintering time for the 5 samples listed in Table V. This calculation involved a ramping of the temperature and pressure from 0.1MPa and 293K at t=0s to 15.168MPa and 973K at t=500s. Holding the temperature and pressure constant for 3600s and then ramping down to ambient conditions in 500s.